01 Apr 2002

Doubly Differential Electron-Emission Spectra in Single and Multiple Ionization of Noble-Gas Atoms by Fast Highly-Charged-Ion Impact

Tom Kirchner

Laszlo Gulyas

Robert Moshammer

Michael Schulz
Missouri University of Science and Technology, schulz@mst.edu

et. al. For a complete list of authors, see https://scholarsmine.mst.edu/phys_facwork/1305

Recommended Citation

T. Kirchner et al., "Doubly Differential Electron-Emission Spectra in Single and Multiple Ionization of Noble-Gas Atoms by Fast Highly-Charged-Ion Impact," *Physical Review A. Atomic, Molecular, and Optical Physics*, vol. 65, no. 4, pp. 427271-427279, American Physical Society (APS), Apr 2002.
The definitive version is available at https://doi.org/10.1103/PhysRevA.65.042727

Doubly differential electron-emission spectra in single and multiple ionization of noble-gas atoms by fast highly-charged-ion impact

T. Kirchner,[1] L. Gulyás,[2] R. Moshammer,[3] M. Schulz,[4] and J. Ullrich[3]
[1]*Department of Physics and Astronomy, York University, Toronto, Ontario, Canada M3J 1P3*
[2]*Institute of Nuclear Research of the Hungarian Academy of Sciences (ATOMKI), P.O. Box 51, H-4001 Debrecen, Hungary*
[3]*Max-Planck-Institute für Kernphysik, Saupfercheckweg 1, 69117 Heidelberg, Germany*
[4]*Department of Physics, University of Missouri-Rolla, Rolla, Missouri 6540*
(Received 1 November 2001; revised manuscript received 22 January 2002; published 10 April 2002)

Low-energy electron emission spectra are studied in collisions of 3.6 MeV/amu Au^{53+} ions with neon and argon atoms for well-defined degrees of target ionization. We calculate doubly differential cross sections as functions of the recoil-ion charge state in the continuum-distorted-wave with eikonal initial-state approximation using a binomial analysis of the total and differential ionization probabilities, and compare them with the present and with previously published experimental data. Very good agreement is found for the single-ionization spectra and for double ionization of neon, while some discrepancies are observed in the spectra for double and triple ionization of argon.

DOI: 10.1103/PhysRevA.65.042727 PACS number(s): 34.50.Fa

I. INTRODUCTION

By combining recoil-ion momentum spectroscopy with highly efficient electron spectrometers it has recently become possible to map the low-energy electron continuum of atoms subject to ionizing collisions of charged particles or photons down to threshold [1]. In particular, several kinematically complete experiments have been carried out for single [2], double [2,3], and triple [4] ionization of atoms by fast-ion impact. These measurements have provided important insights into the collision dynamics, e.g., different ionization mechanisms were identified, and the role of electron-electron correlations in multiple-electron transitions was analyzed to some extent [5].

A deeper understanding of the data hinges on the availability of systematic theoretical models for the description of the investigated scattering systems. For 100 MeV/amu C^{6+} + He collisions a combined experimental and theoretical study of single ionization revealed the importance of higher-order contributions to electron ejection in the plane that is perpendicular to the scattering plane and contains the initial projectile beam direction [6]. In the case of double ionization a comparison of experimental spectra with calculations in the first Born approximation with shake-off elucidated the role of initial- and final-state correlation effects on a detailed level [7]. In the regime of strong perturbations $Q_P/v_P>1$ (Q_P and v_P are the charge and the velocity of the projectile, respectively) experimental doubly differential electron-emission spectra for single ionization revealed strong two-center effects even at very low electron energies and a peak at ultralow energies, which was termed the ''target cusp'' [8,9]. Both features could be reproduced by continuum-distorted-wave with eikonal initial-state (CDW-EIS) calculations reported along with the measurements. By contrast, first-order Born calculations fail to describe the data in this region [10]. This demonstrates that higher-order contributions are important to describe the two-center nature of the electron emission for $Q_P/v_P>1$, and that they are efficiently included in the CDW-EIS model.

We note that very recently marked discrepancies between experiment and CDW-EIS calculations were found in electron spectra as a function of the projectile deflection when the Coulomb interaction between the fast, highly charged projectile and the target nuclei is omitted in the calculation [11,12]. The inclusion of the nucleus-nucleus interaction changes the theoretical results significantly, but does not remove the discrepancy with the experimental data [11,13]. This result is in contrast with previous calculations for intermediate energy proton-helium collisions [14], which demonstrated that the inclusion of the nucleus-nucleus interaction improves the agreement with experiment [15] considerably. While this issue is not yet settled satisfactorily, we emphasize that doubly differential cross sections (DDCS's) for electron emission, which are integrated over the projectile scattering angle, are not affected by the interaction between the nuclei [16]. The present paper deals only with DDCS's of this type.

The CDW-EIS calculations reported for helium [8], neon, and argon [9] target atoms rely on an effective single-particle picture; i.e., the target atom is represented by a single-particle potential, and transition amplitudes to continuum states are calculated for all initially occupied orbitals. For neon and argon targets the theoretical single-particle electron-emission spectra show a marked dependence on the individual initial states, but these structures disappear when the contributions of all initial states are added to compare the spectra with experimental DDCS's [10]. It has been pointed out that the results obtained by this summation do not correspond to pure single ionization, but to *inclusive* or net ionization events, i.e., to situations in which the final state of one electron in the continuum is detected, while nothing is known about the final states of the other electrons [17]. As the latter can also be removed from the target in the same collision event, the net ionization DDCS contains contributions from multiple ionization processes. This interpretation of the theoretical results is supported by the fact that im-

proved agreement between theory and experiment at higher ejected electron velocities was found when the experimental DDCS's for single- and multiple-electron ionization events were added according to the degree of ionization [9].

Given these findings the question arises whether it is possible to extract theoretical DDCS's for a *given* final charge state q of the recoil ion from the CDW-EIS calculations in order to compare theory and experiment in more detail. Such DDCS's are still one-electron spectra, but they are obtained in coincidence with multiple ionization in the case of $q>1$. This problem is addressed in the present paper. We are particularly interested in the question of whether such spectra can be described in the framework of the independent-particle model (IPM). We concentrate on 3.6 MeV/amu Au^{53+} impact on neon and argon targets, for which good agreement between experiment and the CDW-EIS calculations was found for the net electron emission. A preliminary account of this work including theoretical results for neon targets was given in Ref. [18].

The present paper is organized as follows. We start with a brief summary of the CDW-EIS model in Sec. II A, and we describe in Sec. II B an IPM-based analysis used to calculate the DDCS as a function of the recoil-ion charge state q. In Sec. III we compare the calculations with experimental data for neon (Sec. III A) and argon (Sec. III B) targets. Our findings are summarized in Sec. IV. Atomic units ($\hbar=m_e=e=1$) are used throughout.

II. THEORY

A. CDW-EIS model for net electron emission

In the effective single-particle description of ion collisions with multielectron target atoms the scattering system is represented by a set of time-dependent single-particle equations for all initially occupied orbitals,

$$i\partial_t\psi_i(\mathbf{r},t)=\hat{h}(t)\psi_i(\mathbf{r},t), \quad i=1,\ldots,N. \tag{1}$$

We use a Hamiltonian in which the Coulombic electron-nucleus and electron-electron interactions in the target atom are taken into account in terms of a frozen atomic potential v_{atom}. The projectile is located at the position $\mathbf{R}$ with respect to the target center, and is described by a pure Coulomb potential for the charge Q_P ($Q_P=53$ in the present case of Au^{53+} projectile ions)

$$\hat{h}(t)=-\frac{1}{2}\Delta+v_{\text{atom}}(r)-\frac{Q_P}{|\mathbf{r}-\mathbf{R}|}. \tag{2}$$

Recent studies have shown that it is important to employ accurate atomic potentials v_{atom} in order to obtain reasonable electron-emission spectra [17]. In this work we use the exchange-only version of the optimized potential method (OPM) [19], in which self-interaction contributions contained in the Hartree potential are canceled exactly by the exchange term such that the correct asymptotic $-1/r$ behavior is approached smoothly.

In the CDW-EIS model introduced by Crothers and McCann [20] the single-particle equations (1) are solved to first order of a distorted-wave series. The transition amplitudes to final continuum states can be written as

$$a_{if}(\mathbf{b})=-i\int_{-\infty}^{+\infty}dt\langle\chi_f^-|\hat{h}-i\partial_t|\chi_i^+\rangle, \tag{3}$$

where $\mathbf{b}$ denotes the impact-parameter vector, and χ_i^+ and χ_f^- are the distorted initial and final states, respectively. They are taken to be products of undisturbed eigenfunctions $\varphi_{i,f}$ of the target atom and distortion factors $\mathcal{L}_{i,f}^{\pm}$ which account for the interaction of the active electron with the projectile,

$$\chi_i^+=\varphi_i(\mathbf{r})\mathcal{L}_i^+(\mathbf{r}-\mathbf{R})e^{-i\varepsilon_i t}, \tag{4}$$

$$\chi_f^-=\varphi_f(\mathbf{r})\mathcal{L}_f^-(\mathbf{r}-\mathbf{R})e^{-i\varepsilon_f t}. \tag{5}$$

With this ansatz two-center effects are included in the description of the scattering system while the first Born approximation is obtained by setting $\mathcal{L}_i^+=\mathcal{L}_f^-=1$.

The undisturbed bound and continuum functions $\varphi_{i,f}$ are obtained from a numerical solution of the stationary Schrödinger equation for the target atom with the OPM potential [21]. The initial-state distortion factor $\mathcal{L}_i^+$ is given by an eikonal phase, whereas the final-state distortion factor $\mathcal{L}_f^-$ is represented by a Coulomb wave. These choices define the CDW-EIS model and ensure that the boundary conditions of the scattering system with long-range Coulomb potentials are satisfied [22].

Instead of calculating the integral of Eq. (3) explicitly one makes use of the fact that the Fourier transform $R_{if}(\boldsymbol{\eta})$ of $a_{if}(\mathbf{b})$ can be given in analytic form [21]. DDCS's for net ionization as a function of the energy ε_{el} and solid angle Ω_{el} of the ejected electron are obtained by integrating $|R_{if}|^2$ over the transverse momentum transfer $\boldsymbol{\eta}$ and summing up the contributions of all initially occupied orbitals,

$$\frac{d^2\sigma}{d\varepsilon_{\text{el}}d\Omega_{\text{el}}}=\sum_{i=1}^{N}\int d^2\eta|R_{if}(\boldsymbol{\eta})|^2=\sum_{i=1}^{N}\int d^2b|a_{if}(\mathbf{b})|^2. \tag{6}$$

B. CDW-EIS model for electron emission for a given recoil-ion charge state

As a first step for the calculation of electron-emission spectra as a function of the recoil-ion charge state q we extract the impact-parameter-dependent ionization amplitudes $a_{if}(\mathbf{b})$ by evaluating the two-dimensional Fourier transform

$$a_{if}(\mathbf{b})=\frac{1}{2\pi}\int d\boldsymbol{\eta}\exp(-i\boldsymbol{\eta}\cdot\mathbf{b})R_{if}(\boldsymbol{\eta}). \tag{7}$$

Details of this procedure can be found in Ref. [23]. We define the single-particle probability for the transition from a given initial state to a final state with emission energy ε_{el} and emission angle Ω_{el} by

$$\frac{d^2p_i(b)}{d\varepsilon_{\text{el}}d\Omega_{\text{el}}}=\frac{1}{2\pi}\int_0^{2\pi}d\varphi_b|a_{if}(\mathbf{b})|^2, \tag{8}$$

where φ_b denotes the azimuthal angle of the impact-parameter vector **b**. Total single-particle ionization probabilities are obtained by integrating Eq. (8) over the electron coordinates,

$$p_i(b)=\int d\varepsilon \int d\Omega_{\rm el}\frac{d^2p_i(b)}{d\varepsilon d\Omega_{\rm el}}. \tag{9}$$

Furthermore, we define the integrated net ionization probability by

$$P_{\rm net}(b)=\sum_{i=1}^{N} p_i(b). \tag{10}$$

This quantity corresponds to the average number of emitted electrons and is equal to the mean value of the distribution of the probabilities P_q for the ionization of q out of N electrons:

$$P_{\rm net}(b)=\sum_{q=1}^{N} qP_q(b). \tag{11}$$

In the framework of the independent particle model the probabilities P_q for q-fold ionization are calculated by a binomial analysis of the single-particle probabilities p_i. On the level of a shell-specific model [24] P_q is given by

$$P_q(b)=\sum_{q_1,\ldots,q_m=0;q_1+\cdots+q_m=q}^{N_1,\ldots,N_m}\prod_{i=1}^{m}\frac{N_i!}{q_i!(N_i-q_i)!}\times[p_i(b)]^{q_i}[1-p_i(b)]^{N_i-q_i}. \tag{12}$$

Here, m is the number of electron shells, N_i is the initial number of electrons in each shell, and the q_i count the electrons that are removed from the ith shell. Total cross sections (TCS's) for q-fold ionization are obtained by integration of $bP_q(b)$ over the impact parameter b.

In analogy with Eq. (12) one can define *differential* probabilities for q-fold ionization [25]. Here we consider the probability of ionizing q out of N electrons and detecting one of these electrons at the emission energy $\varepsilon_{\rm el}$ and the emission angle $\Omega_{\rm el}$:

$$\frac{d^2P_q(b)}{d\varepsilon_{\rm el}d\Omega_{\rm el}}=\sum_{q_1,\ldots,q_m=0;q_1+\cdots+q_m=q}^{N_1,\ldots,N_m}\prod_{i=1}^{m}\frac{d^2P_{q_i}(b)}{d\varepsilon_{\rm el}d\Omega_{\rm el}}, \tag{13}$$

$$\frac{d^2P_{q_i}(b)}{d\varepsilon_{\rm el}d\Omega_{\rm el}}=\frac{N_i!}{q_i!(N_i-q_i)!}\frac{d^2p_i(b)}{d\varepsilon_{\rm el}d\Omega_{\rm el}}[p_i(b)]^{q_i-1}\times[1-p_i(b)]^{N_i-q_i}. \tag{14}$$

Integration of this differential probability over the impact parameter b yields the DDCS for well-defined degrees of ionization q. The total q-fold ionization probability P_q [Eq. (12)] is recovered when Eq. (13) is integrated over $\varepsilon_{\rm el}$ and $\Omega_{\rm el}$. Finally, we define a differential net ionization probability in analogy with Eq. (10) and obtain

$$\frac{d^2P_{\rm net}(b)}{d\varepsilon_{\rm el}d\Omega_{\rm el}}=\sum_{i=1}^{N}\frac{d^2p_i(b)}{d\varepsilon_{\rm el}d\Omega_{\rm el}}=\sum_{q=1}^{N} q\frac{d^2P_q(b)}{d\varepsilon_{\rm el}d\Omega_{\rm el}}. \tag{15}$$

This quantity measures the impact-parameter-dependent probability of finding an electron with emission energy $\varepsilon_{\rm el}$ and emission angle $\Omega_{\rm el}$ in the continuum, while the other electrons are not detected. When integrated over b the DDCS of Eq. (6) is obtained again.

III. RESULTS AND DISCUSSION

In this section we compare our theoretical results with present and with previously published experimental data for 3.6 MeV/amu Au^{53+} impact on neon (Sec. III A) and argon (Sec. III B) atoms [9]. In addition to the CDW-EIS model we have used the nonperturbative basis generator method (BGM) [26] to calculate total probabilities and cross sections for electron removal (the sum of ionization and capture) from neon targets. These data are included in the discussion to provide some additional information about the quality of the CDW-EIS approximation in the regime of strong perturbations ($Q_P/v_P\approx 4.4$ a.u. for the present collision systems).

In the BGM, the single-particle equations (1) are solved in a dynamically adapted basis constructed by repeated application of the (regularized) projectile potential on a set of undisturbed target eigenstates $\{|\varphi_v\rangle, v=1,\ldots,V\}$. The basis does not include moving projectile states explicitly to describe electron capture, but previous work has shown that capture and ionization can be separated by projecting out the part of the electronic density that is transferred to the projectile [27]. In the present calculations we have not carried out these projections, since a large number of states has to be considered for the 53-fold charged projectile, and capture can be expected to be small in the fast collisions considered here ($v=12$ a.u.). Therefore, the electron removal cross sections should be comparable with the ionization cross sections. We have used the same basis set as in Ref. [27].

The experiments were performed at the Universal Accelerator (UNILAC) of GSI (Gesellschaft für Schwerionenforschung) using a multielectron recoil-ion momentum spectrometer. Details about the operating principle and the resolution of the spectrometer can be found in Ref. [28]. Electron spectra for emission energies $\varepsilon_{\rm el}=100$ eV down to threshold ($\varepsilon_{\rm el}=0$ eV) have been measured in coincidence with the full momentum vector and the charge state of the recoiling target ion, and the (unchanged) charge state of the outgoing projectile to obtain DDCS's for well-defined degrees of ionization. An electron momentum resolution of $\Delta p_{\parallel}=1\times10^{-2}$ a.u. in the longitudinal and $\Delta p_{\perp}=1.4\times10^{-2}$ a.u. in the transverse direction with respect to the projectile beam axis has been achieved. This corresponds to an energy resolution of $\Delta\varepsilon_{\rm el}=2.5$ meV at threshold. For each event the momentum vectors of up to three electrons were recorded yielding kinematically complete experiments of single, double, and triple ionization. In this paper we concentrate on one-electron spectra for well-defined degrees of

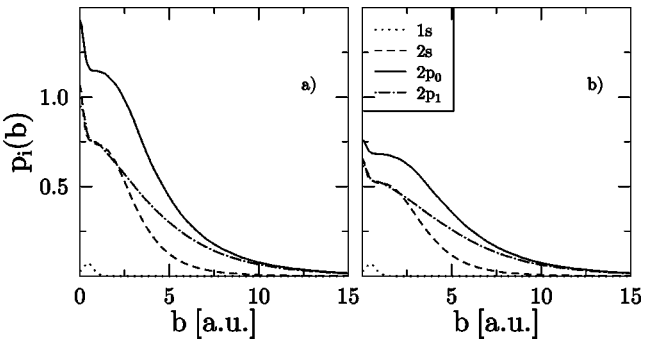

FIG. 1. Single-particle ionization probabilities for the $1s$, $2s$, and $2p$ initial states as functions of the impact parameter for 3.6 MeV/amu $Au^{53+}+Ne$ collisions. (a) Original CDW-EIS calculations and (b) CDW-EIS calculations using Eq. (17).

ionization, which are integrated over the deflection of the projectile. Kinematically complete data for single ionization of helium are reported in Ref. [12].

A. The collision system 3.6 MeV/amu $Au^{53+}+Ne$

For the collision systems to be discussed in this paper we encounter the problem that the integrated single-particle ionization probabilities $p_i(b)$ [Eq. (9)] become large at small impact parameters b and exceed unity for some initial states. This behavior is a consequence of the nonunitarity of the CDW-EIS approximation, and shows the limited validity of this perturbative method for close collisions, in which the perturbation is very large. We note, however, that the CDW-EIS model has proven to be valid in the strong perturbation regime as long as the region in which the probabilities exceed unity is relatively small [29]. This is due to the fact that higher-order effects are efficiently included in the distorted initial and final states.

In order to use the calculated $p_i(b)$ in the binomial analysis of differential and total ionization cross sections one has to ensure that $p_i(b)\leqslant 1$ for all b, since otherwise some multiple-electron probabilities become negative. We have considered two alternative methods: first, we have capped the $p_i(b)$ [model (a)]

$$\tilde{p}_i(b)=1 \quad \text{if} \quad p_i(b)>1, \tag{16}$$

and, second, we have used the unitarization prescription proposed in Ref. [30] [model (b)]

$$\tilde{p}_i(b)=1-\exp[-p_i(b)]. \tag{17}$$

In Fig. 1 we show the original and the unitarized single-particle ionization probabilities for neon target atoms. The largest contribution to the total cross section is due to the $2p_0$ initial state, which is aligned along the projectile beam direction. The corresponding probability p_{2p_0} exceeds unity for impact parameters $b\leqslant 2.4$ a.u. The contribution from the $2s$ initial state exceeds unity only slightly at very small impact parameters $b\leqslant 0.1$ a.u., while the ionization probability of the perpendicularly aligned $2p_1$ initial state remains smaller than 1 at all b values. The $1s$ initial state is ionized

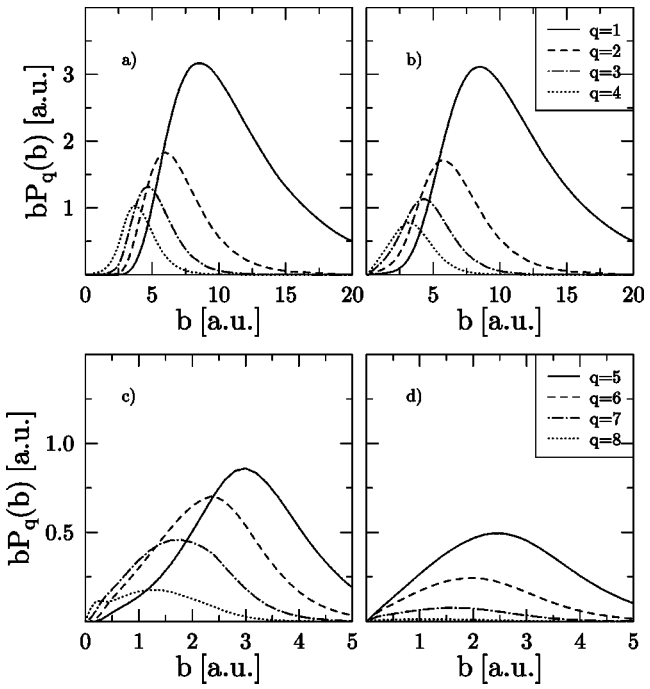

FIG. 2. Impact-parameter-weighted probabilities for q-fold ionization as functions of the impact parameter for 3.6 MeV/amu $Au^{53+}+Ne$ collisions. CDW-EIS calculations for $q=1,\ldots,4$ using (a) Eq. (16) and (b) Eq. (17), and CDW-EIS calculations for $q=5,\ldots,8$ using (c) Eq. (16) and (d) Eq. (17).

only weakly due to its strong binding energy. The unitarized probabilities of the initial L-shell states are considerably smaller than the original probabilities in the impact-parameter range $0\leqslant b\leqslant 5$ a.u., and approach them at larger b. We note that we have applied Eq. (17) to all initial states, since we find it more consistent to assume that the probabilities which are slightly smaller than 1 are also overestimated to some extent.

The impact-parameter-weighted total probabilities for q-fold ionization $bP_q(b)$ obtained from model (a) [Eq. (16)] and model (b) [Eq. (17)] are displayed in Fig. 2. Obviously, the probabilities associated with higher recoil-ion charge states are significantly reduced by the unitarization. They contribute mainly at small impact parameters, for which the unitarization depletes the single-particle probabilities. We also observe that the $bP_q(b)$ for the lower charge states are shifted somewhat toward smaller values of b. Model (a) [Eq. (16)] forbids one-electron ionization rigorously and two-electron ionization very efficiently in the $b\leqslant 2.4$ a.u. range, in which the ionization probability of the $2p_0$ initial state is set equal to 1. This is a consequence of the $(1-p_{2p_0})^{2-q_i}$ factors in Eq. (12). In model (b) [Eq. (17)] this condition is relaxed, and one- and twofold ionization events are possible in close collisions, albeit with small probabilities.

In Fig. 3 we compare the TCS's for q-fold ionization σ_q of neon atoms obtained from model (a) and model (b) with experimental data and q-fold electron removal cross sections obtained from the BGM, in which unitarity is ensured automatically. Since the experimental cross sections were not measured on an absolute scale we have plotted the ratios

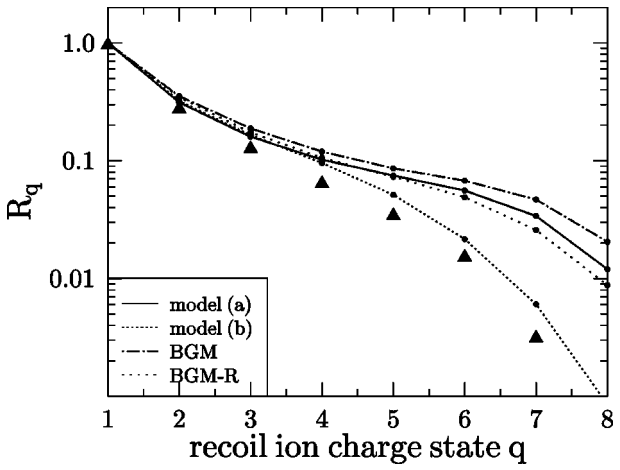

FIG. 3. Total cross section ratio $R_q=\sigma_q/\sigma_1$ as a function of the recoil-ion charge state q for 3.6 MeV/amu $Au^{53+}+Ne$ collisions. The theoretical models are explained in the text. Full triangles: present experimental data.

$R_q=\sigma_q/\sigma_1$ in Fig. 3. First, we notice that the CDW-EIS calculations with both models (a) and (b) give almost identical results for the lower charge states $q\leqslant 4$. These charge states are mainly produced in relatively distant collisions, in which the single-particle probabilities of both models are very similar (cf. Fig. 2). At higher q the unitarization reduces the TCS significantly and leads to good agreement with the experimental data, while model (a) badly overestimates the measurements in this range. One is led to the conclusion that the unitarization improves the quality of the CDW-EIS approximation for the large perturbation $Q_P/v_P\approx 4.4$ a.u. However, the cross sections obtained from the BGM support the results of model (a), and are even larger for the highest charge states q, since the K-shell electrons are efficiently removed from the target atom by capture processes occurring in close collisions. The comparison of the CDW-EIS and BGM results favors a different interpretation, namely, that model (b) overemphasizes the effect of unitarity, and that model (a) is better suited to correct the original CDW-EIS results. If one adopts this point of view, one has to conclude that the experimental data cannot be described by the Hamiltonian (2) and the binomial analysis (12) of the propagated orbitals, and that the good agreement of model (b) with the experimental data is fortuitous.

To improve the description of the scattering system we have repeated the BGM calculations with a Hamiltonian that includes time-dependent screening effects due to the increasing binding of the target as electrons are removed during the collision (BGM-R). We have used the global screening model proposed in Ref. [31]. Figure 3 shows that time-dependent screening reduces the q-fold electron loss cross sections at high q, but the effect is relatively small and does not explain the steep decrease of the experimental data. Given this set of theoretical results it remains unclear whether the measurements at high charge states q can be described in the framework of the IPM using a more refined dynamical screening model, or whether electron correlation has to be taken into account. From the striking agreement of the CDW-EIS results of model (b) and experiment one may

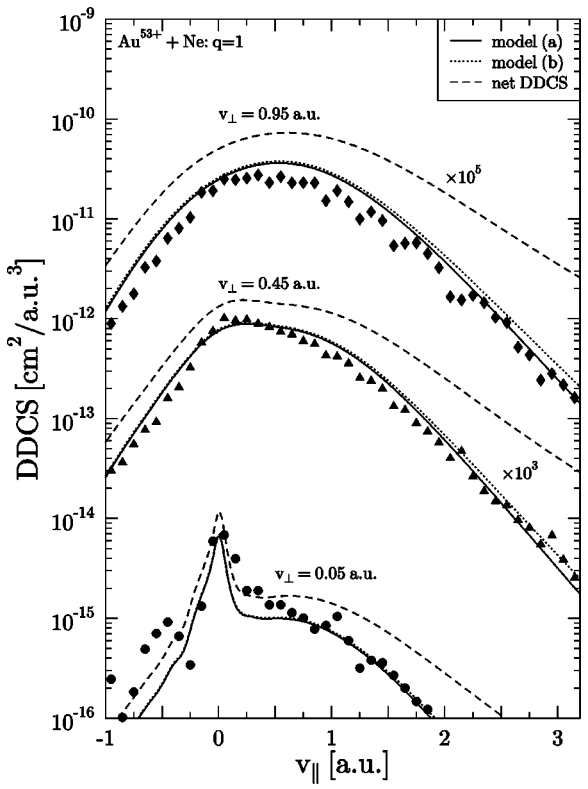

FIG. 4. DDCS's for net and single ($q=1$) electron emission in 3.6 MeV/amu $Au^{53+}+Ne$ collisions. The DDCS's at $v_\perp=0.45$ and 0.95 a.u. are multiplied by the indicated factors. Model (a) refers to the use of Eq. (16), model (b) to Eq. (17). Symbols: experimental data from Ref. [9] normalized to the present CDW-EIS calculations for $q=1$.

speculate that the unitarization mimics effects that are beyond the IPM, but further studies are necessary to clarify this issue. Obviously, it would also be desirable to perform similar comparisons between theory and experiment in the regime of weaker perturbations Q_P/v_P, in which no *ad hoc* corrections of the single-particle ionization probabilities such as the unitarization procedure are necessary.

We now turn to the DDCS's for well-defined degrees of ionization. In Fig. 4 we compare theoretical results for net and single (i.e., $q=1$) ionization of neon with the experimental DDCS's for $q=1$ that were published in Ref. [9]. As can be expected from the total ionization probabilities (Fig. 2) the results obtained from both models (a) and (b) essentially coincide. They are in very good agreement with the experimental DDCS's over the entire range of transverse and longitudinal electron emission velocities shown. Only for the lowest transverse velocity cut at $v_\perp=0.05$ a.u. do we observe slight discrepancies around longitudinal velocities $v_\parallel\approx 0.25$ a.u. The fact that we have confined the calculation of probabilities to impact parameters $b\leqslant 20$ a.u. is likely to explain why the calculated DDCS is smaller than the experimental one in this region of low emission velocities that corresponds to distant collisions.

The theoretical results for net ionization, which are also included in Fig. 4, are in close agreement with earlier calculations for $Au^{53+}+Ne$ collisions [9] obtained with a Hartree-

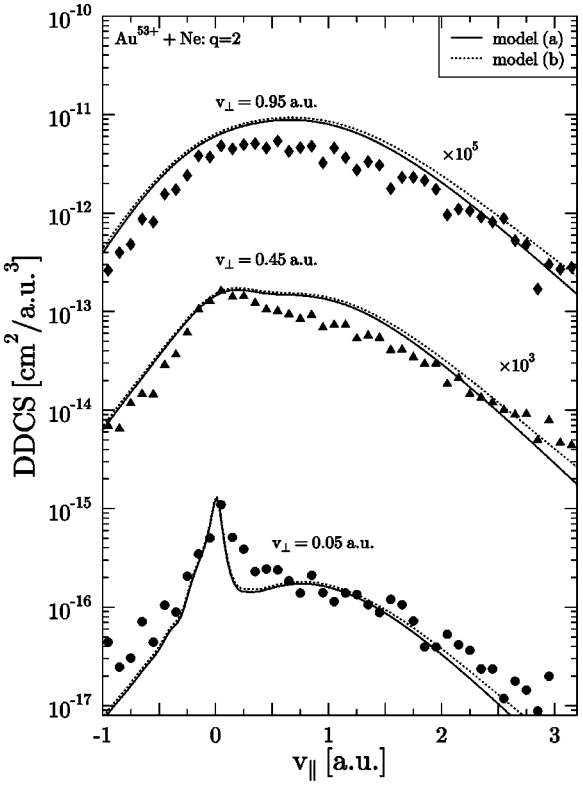

FIG. 5. DDCS's for double ($q=2$) electron emission in 3.6 MeV/amu $Au^{53+}+Ne$ collisions. The DDCS's at $v_\perp=0.45$ and 0.95 a.u. are multiplied by the indicated factors. Model (a) refers to the use of Eq. (16), model (b) to Eq. (17). Symbols: present experimental data. The measurements have been put on an absolute scale by using the measured ratio $R_2=\sigma_2/\sigma_1$ and the normalization of the DDCS for $q=1$ to the present CDW-EIS calculations.

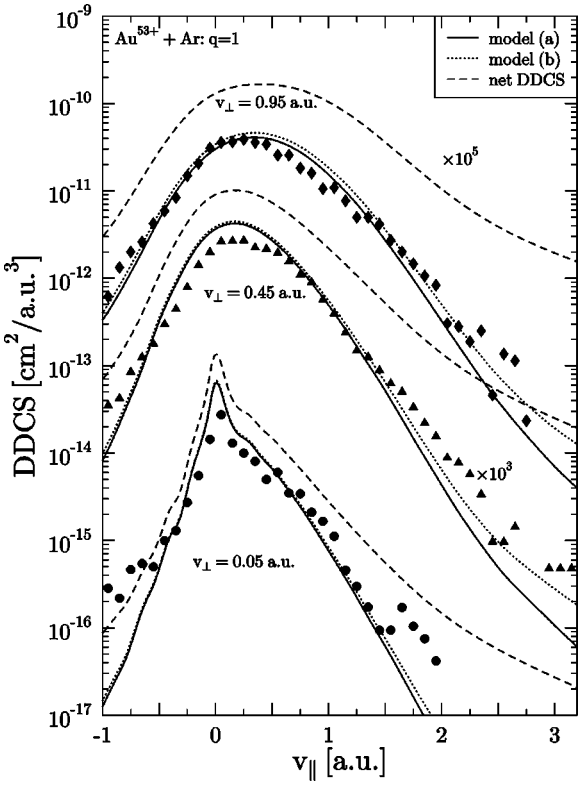

FIG. 6. DDCS's for net and single ($q=1$) electron emission in 3.6 MeV/amu $Au^{53+}+Ar$ collisions. The DDCS's at $v_\perp=0.45$ and 0.95 a.u. are multiplied by the indicated factors. Model (a) refers to the use of Eq. (16), model (b) to Eq. (17). Symbols: experimental data from Ref. [9] normalized to the present CDW-EIS calculations for $q=1$.

Fock-Slater model potential to describe the target atom (see also Ref. [18]). We observe that the net DDCS falls off more flatly at higher longitudinal emission velocities $v_\parallel$ than the DDCS for $q=1$. This behavior reflects the contributions of multiple-ionization events in close collisions, which correspond to relatively high emission velocities.

Figure 5 displays the DDCS's obtained in coincidence with the recoil-ion charge state $q=2$. Again, the results of model (a) and model (b) to correct the single-particle probabilities are in close agreement. Model (b) leads to slightly larger DDCS's, particularly at higher $v_\parallel$. This can be explained by the fact that twofold ionization is not as efficiently suppressed in model (b) as in model (a) in the region of small impact parameters (cf. Fig. 2), which gives rise predominantly to relatively fast emitted electrons. The agreement with the experimental data is very good, which demonstrates that DDCS's corresponding to low charge states q can be reliably calculated in the IPM framework for neon atoms. Given the TCS's shown in Fig. 3 we expect discrepancies in the DDCS's at higher charge states, when model (a) is used. It would be interesting to check whether model (b) would improve this situation as for the TCS's of Fig. 3, but, unfortunately, the statistics are not sufficient to extract experimental DDCS's in coincidence with higher q values.

B. The collision system 3.6 MeV/amu $Au^{53+}+Ar$

For argon targets the single-particle ionization probabilities of all M-shell electrons exceed unity at small impact parameters b with maximum values that are larger than in the case of neon. This can be explained by the smaller binding energies of the argon states, which make ionization more likely. The $3p_0$ initial state gives the largest contribution to the total ionization cross section. The corresponding probability p_{3p_0} exceeds unity for $b\leqslant 3.3$ a.u., and reaches the value $p_{3p_0}=1.64$ at $b=0$ a.u. The $3s$- and $3p_1$-state probabilities exceed unity only at small impact parameters $b<0.3$ a.u.

As in the case of neon targets we have applied the IPM-based analysis of Sec. II B and model (a) [Eq. (16)] and model (b) [Eq. (17)] in order to calculate the DDCS as a function of the recoil-ion charge state q [Eq. (13)]. The results for $q=1$ are presented in Fig. 6. Both models give similar results except for high longitudinal velocities $v_\parallel$, for which the DDCS's obtained from model (b) are somewhat larger. This behavior is also present for neon targets (cf. Fig. 4), but it is much more pronounced in the case of argon, since the impact-parameter region in which the single-particle ionization probabilities become larger than 1 is extended to larger b values. As a consequence, the total one-electron ionization probability ($P_{q=1}$) equals zero in model

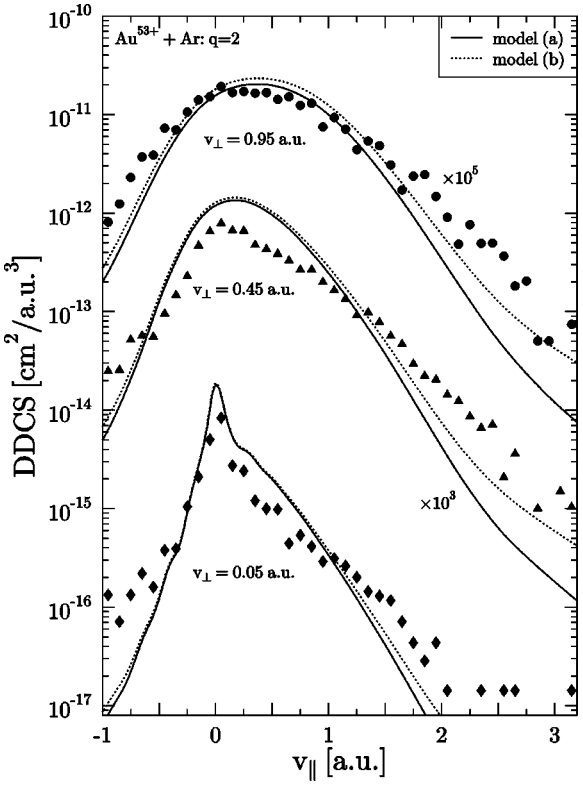

FIG. 7. DDCS's for double ($q=2$) electron emission in 3.6 MeV/amu Au^{53+} + Ar collisions. The DDCS's at $v_\perp=0.45$ and 0.95 a.u. are multiplied by the indicated factors. Model (a) refers to the use of Eq. (16), model (b) to Eq. (17). Symbols: present experimental data normalized to the present CDW-EIS calculations for $q=2$.

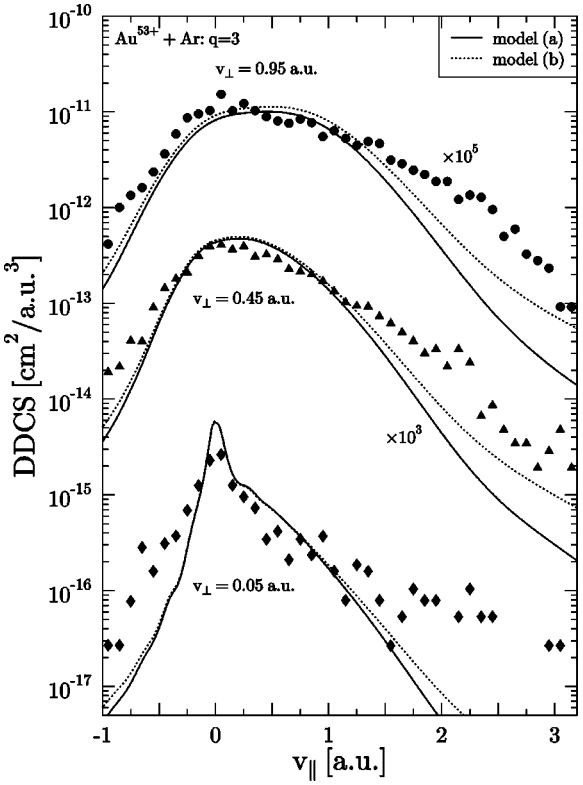

FIG. 8. DDCS's for triple ($q=3$) electron emission in 3.6 MeV/amu Au^{53+} + Ar collisions. The DDCS's at $v_\perp=0.45$ and 0.95 a.u. are multiplied by the indicated factors. Model (a) refers to the use of Eq. (16), model (b) to Eq. (17). Symbols: present experimental data normalized to the present CDW-EIS calculations for $q=3$.

(a) over a larger range of impact parameters, whereas this process has a nonzero probability if model (b) is applied. We find very good agreement with the experimental data for the transverse velocity cuts $v_\perp=0.05$ a.u. and $v_\perp=0.95$ a.u., and a theoretical DDCS that decreases somewhat more rapidly than the measurements at $v_\perp=0.45$ a.u. in the region of larger longitudinal velocities $v_\parallel$. We note that this discrepancy is slightly reduced when model (b) is applied to calculate the DDCS.

We have also included the theoretical results for net ionization in Fig. 6, which were compared to experimental DDCS's summed over the degree of ionization in Ref. [9]. The deviations of the net DDCS's from the DDCS's for $q=1$ are significantly larger than for neon targets, since multiple-ionization events occur with higher probability in the case of argon. This observation shows clearly that the net DDCS, which is obtained by summing over the contributions of all initial states [Eq. (6)] should not be compared with experimental single ($q=1$) ionization. Only for weak perturbations Q_P/v_P does this procedure avoid significant errors, since the contributions from multiple-ionization events are small.

In Fig. 7 we present DDCS's for $q=2$. As the ratio of the DDCS's for double to those for single ionization could not be determined with sufficient accuracy from the measurements, we have adjusted the absolute normalization of the experimental data to the theoretical results. We observe comparable shapes of the measured and calculated DDCS's, but we note that better agreement was found for double ionization of neon (cf. Fig. 5). Similar to the case of $q=1$ the DDCS's obtained from model (b) fall off more flatly at higher longitudinal velocities $v_\parallel$ than the results of model (a), a trend that is supported by the experimental data and is also observed in the DDCS's for $q=3$ (Fig. 8). Obviously, the experimental uncertainty is larger than for the lower charge states q, but the data indicate even more flatly decreasing DDCS's at higher values of $v_\parallel$ than predicted by the CDW-EIS calculations using model (b) for all transverse velocity cuts.

Finally, we present theoretical DDCS's obtained from model (a) for $q=1,\ldots,8$ at $v_\perp=0.05$ in Fig. 9. We observe that the asymmetry of the DDCS increases with increasing charge state q. This feature can be attributed to two-center (postcollision interaction) effects, since higher q values are mainly produced in close collisions (cf. Fig. 2), in which the projectile drags the electrons strongly in the forward direction. We note that this two-center effect is also observed at higher transverse velocities.

Interestingly, the DDCS's for $q=1,\ldots,6$ cross at a single point located at $v_\parallel\approx 2$ a.u. A detailed analysis of the differential and total single-particle probabilities involved in forming the DDCS shows that the crossing is caused by the exponential decay of the probabilities at large impact parameters b and the binomial expression (13) to calculate

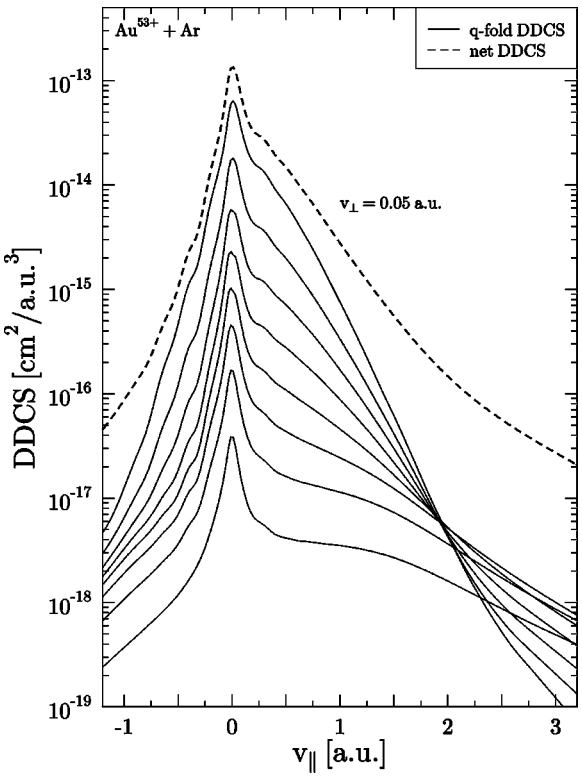

FIG. 9. DDCS's for net and q-fold electron emission in 3.6 MeV/amu Au^{53+} + Ar collisions at $v_\perp = 0.05$ a.u. The DDCS's for the charge states q correspond to $q = 1, \ldots, 8$ from top to bottom at the locations of the maxima.

the DDCS, i.e., it is a direct consequence of the IPM-based analysis. We found that such crossings are present in the theoretical spectra in a variety of different situations; i.e., they occur also for higher transverse velocities, for weaker perturbations, and for the other target atoms. When model (b) is applied to correct the single-particle probabilities the crossings are located at slightly smaller longitudinal velocities $v_\parallel$ than in the case of model (a). They are shifted to larger values of $v_\parallel$ when the perturbation strength is decreased. Only for perturbations as large as in the present case are they located at electron velocities that are in principle accessible in multielectron recoil-ion momentum spectroscopy experiments. Unfortunately, the present data exhibit relatively large uncertainties in the $v_\parallel$ region of interest, and, as stated above, the ratios of the DDCS's for different charge states q were not determined with sufficient accuracy to perform this comparison. It would be very interesting to check the theoretical prediction in a future experiment, as this would give direct information about the validity of the present approach to calculating DDCS's for well-defined degrees of ionization in the framework of the IPM.

IV. CONCLUDING REMARKS

In this work we have considered differential and total ionization cross sections for given recoil-ion charge states q. We have calculated impact-parameter-dependent ionization probabilities for 3.6 MeV/amu Au^{53+} impact on neon and argon atoms with the CDW-EIS method and have used a binomial analysis to extract DDCS's and TCS's as functions of q. Good agreement with experimental DDCS's is found for single ionization. The single-ionization DDCS's fall off more steeply with increasing longitudinal electron velocity $v_\parallel$ than the net ionization DDCS's, which are obtained by simply summing over all initial target states. This demonstrates clearly that net ionization has to be distinguished from single ionization in the regime of strong perturbations.

Furthermore, we have found that the total single-particle ionization probabilities of the outermost subshells exceed unity at small impact parameters and need to be capped or unitarized. The DDCS's for single and double ionization of neon are rather insensitive to these procedures and agree well with the measurements. However, the TCS's are reduced by the unitarization prescription (17) for the higher recoil-ion charge states such that the agreement with experiment is improved considerably. At present it remains unclear whether this behavior, which is not supported by nonperturbative BGM calculations, is fortuitous. For argon targets the unitarization prescription (17) shifts the total q-fold ionization probabilities to smaller impact parameters and leads to an increase of the DDCS's for $q = 1, \ldots, 3$ at large $v_\parallel$. The agreement with experiment is considerably improved compared to the results obtained from capping the probabilities according to Eq. (16).

From these findings we conclude that DDCS's can be successfully calculated from a binomial analysis of the total and differential CDW-EIS ionization probabilities for low recoil-ion charge states. Future investigations should concentrate on smaller perturbations, for which the problem of unitarization is not present, in order to prove or disprove this conclusion.

ACKNOWLEDGMENTS

We would like to thank M. Horbatsch for helpful discussions. This work was partially supported by GSI, NSF, and the Leibniz-Program of the Deutsche Forschungsgemeinschaft. T.K. gratefully acknowledges the financial support of the DAAD, and L.G. gratefully acknowledges a grant from the J. Bolyai Research Scholarship Foundation.

[1] J. Ullrich *et al.*, J. Phys. B **30**, 2917 (1997); R. Dörner *et al.*, Phys. Rep. **330**, 95 (2000).
[2] R. Moshammer *et al.*, Phys. Rev. Lett. **79**, 3621 (1997).
[3] B. Bapat *et al.*, J. Phys. B **32**, 1859 (1999).
[4] M. Schulz *et al.*, Phys. Rev. A **61**, 022703 (2000).
[5] M. Schulz *et al.*, Phys. Rev. Lett. **84**, 863 (2000).
[6] M. Schulz *et al.*, J. Phys. B **34**, L305 (2001).
[7] B. Bapat, S. Keller, R. Moshammer, and J. Ullrich, J. Phys. B **33**, 1437 (2000); S. Keller, B. Bapat, R. Moshammer, J. Ullrich, and R. M. Dreizler, *ibid.* **33**, 1447 (2000).
[8] W. Schmitt *et al.*, Phys. Rev. Lett. **81**, 4337 (1998).
[9] R. Moshammer *et al.*, Phys. Rev. Lett. **83**, 4721 (1999).

[10] P. D. Fainstein, R. Moshammer, and J. Ullrich, Phys. Rev. A **63**, 062720 (2001).
[11] R. Moshammer *et al.*, Phys. Rev. Lett. **87**, 223201 (2001).
[12] M. Schulz, R. Moshammer, A. N. Perumal, and J. Ullrich, J. Phys. B (to be published).
[13] R. E. Olson and J. Fiol, J. Phys. B **34**, L625 (2001).
[14] V. D. Rodríguez and R. O. Barrachina, Phys. Rev. A **57**, 215 (1998).
[15] M. Schulz *et al.*, Phys. Rev. A **54**, 2951 (1996).
[16] P. D. Fainstein, V. H. Ponce, and R. D. Rivarola, J. Phys. B **21**, 287 (1988); A. Salin, *ibid.* **22**, 3901 (1989).
[17] L. Gulyás, T. Kirchner, T. Shirai, and M. Horbatsch, Phys. Rev. A **62**, 022702 (2000).
[18] T. Kirchner and L. Gulyás, Phys. Scr., T **T92**, 348 (2001).
[19] J. D. Talman and W. F. Shadwick, Phys. Rev. A **14**, 36 (1976); W. Engel and S. H. Vosko, *ibid.* **47**, 2800 (1993).
[20] D. S. F. Crothers and J. F. McCann, J. Phys. B **16**, 3229 (1983).
[21] L. Gulyás, P. D. Fainstein, and A. Salin, J. Phys. B **28**, 245 (1995).
[22] P. D. Fainstein, V. H. Ponce, and R. D. Rivarola, J. Phys. B **24**, 3091 (1991).
[23] P. D. Fainstein, L. Gulyás, and A. Salin, J. Phys. B **29**, 1225 (1996).
[24] M. Horbatsch, Phys. Lett. A **187**, 185 (1994).
[25] P. D. Fainstein and L. Gulyás, J. Phys. B **34**, 3003 (2001).
[26] H. J. Lüdde, A. Henne, T. Kirchner, and R. M. Dreizler, J. Phys. B **29**, 4423 (1996); O. J. Kroneisen, H. J. Lüdde, T. Kirchner, and R. M. Dreizler, J. Phys. A **32**, 2141 (1999).
[27] T. Kirchner, M. Horbatsch, and H. J. Lüdde, Phys. Rev. A **64**, 012711 (2001).
[28] R. Moshammer *et al.*, Nucl. Instrum. Methods Phys. Res. B **108**, 425 (1996).
[29] P. D. Fainstein, L. Gulyás, and A. Dubois, J. Phys. B **31**, L171 (1998).
[30] V. A. Sidorovich and V. S. Nikolaev, J. Phys. B **16**, 3243 (1983).
[31] T. Kirchner, M. Horbatsch, H. J. Lüdde, and R. M. Dreizler, Phys. Rev. A **62**, 042704 (2000).